Breast implant silicone exposure induces immunogenic response and autoimmune markers in human periprosthetic tissue

Isabelle Pluvy, Eve Randrianaridera, Ismail Tahmaz, Martine Melin, Florelle Gindraux, Céline Keime, Arnaud Ponche, Tatiana Petithory, Laurent Pieuchot, Karine Anselme, et al.

Breast implant silicone exposure induces immunogenic response and autoimmune markers in human periprosthetic tissue

Isabelle Pluvy, Eve Randrianaridera, Ismail Tahmaz, Martine Melin, Florelle Gindraux, Céline Keime, Arnaud Ponche, Tatiana Petithory, Laurent Pieuchot, Karine Anselme, et al.

Breast implant silicone exposure induces immunogenic response and autoimmune markers in human periprosthetic tissue

Isabelle Pluvy[1], Eve Randrianaridera[2], Ismail Tahmaz[2], Martine Melin[3], Florelle Gindraux[1,4], Céline Keime[5], Arnaud Ponche[2], Tatiana Petithory[2], Laurent Pieuchot[2], Karine Anselme[2], Isabelle Brigaud[2]

1. Université de Franche-Comté, CHU Besançon, Laboratoire SINERGIES, Service d'orthopédie, traumatologie et chirurgie plastique, F-25000 Besançon, France.
2. Institut de Science des Matériaux de Mulhouse (IS2M), UMR 7361 CNRS/, Université de Haute Alsace (UHA), 15 rue Jean Starcky, 68057, Mulhouse Cedex, France.
3. Novotec, ZAC du Chêne, Europarc, 11 rue Edison, 69500 Bron, France.
4. Orthopaedic, Traumatology and Plastic Surgery Department, University Hospital of Besançon, 25000 Besançon, France.
5. GenomEast platform, IGBMC, CNRS UMR 7104, INSERM U1258, Université de Strasbourg, F-67400 Illkirch, France.
6. Service d'anatomie pathologique, CHU Besançon, F-25000 Besançon, France

Corresponding author: Isabelle Brigaud

Email: isabelle.brigaud@uha.fr

Abstract

Silicone-based breast implants are commonly used, but there are concerns about their long-term safety. While implantation results in the formation of a periprosthetic tissue that isolates the implant from the rest of the host body, silicone can leak and reach surrounding tissues. We combined histological analysis and gene expression profiling (RNA sequencing) of samples from human patients with silicone breast implants with different fillers (silicone or serum), surface topographies and/or shell rupture, and performed systematic cross-comparisons. Our study shows that exposure to silicone gel filler, even in clinically asymptomatic cases, induces an immune response. This response includes the expression of markers associated with various autoimmune diseases. This study provides the first biological evidence of an association between silicone implants and autoimmune markers, highlighting the need for further research and stricter implant safety regulations. We suggest that implant design factors, such as filler type and surface texture, may influence the inflammatory response. Re-evaluation of existing clinical trials is warranted to investigate the association between implant characteristics and potential health risks.

Keywords

breast implant, silicone, human periprosthetic capsule, transcriptome, inflammation, histology

Introduction

Silicone breast implants are the products of decades of research and are designed to support durable and safe implantation[1]. However, since their first introduction in 1962, biological inertness of silicone breast implant remains a recurring and controversial topic. On the one hand, large studies have repeatedly concluded that breast implant are safe, while acknowledging a low rate of complications associated with their use[2,3]. On the other hand, accumulating data

identified silicone exposure as a risk factor to develop a broad spectrum of diseases related to the immune's system response to foreign material, a topic well documented under different acronyms such as BII (Breast Implant Illness)[4–8], "SIIS" (Silicone Implant Incompatibility Syndrome)[9] or "ASIA" (Autoimmune Syndrome Induced Adjuvants)[10,11]. More recently, silicone exposure and associated silicone toxicity have been implicated as factors favoring the development of breast implant-associated anaplastic large cell lymphoma (BIA-ALCL)[12,13], breast implant-associated squamous cell carcinoma (BIA-SCC)[14] and allergic manifestations[15].

Breast implants consist of a highly cross-linked silicone shell with a smooth or textured outer surface, containing a filler (saline, silicone gel or hydrogel) (Fig. 1). Silicone gel is a very lightly cross-linked silicone elastomer whose polymer network has been swollen with silicone fluids. During implantation, the host body unable to eliminate the foreign implant, isolates this exogenous device by synthesizing a fibrous tissue, the periprosthetic capsule, which encapsulates the implant under the control of an immune process known as the foreign body reaction (FBR) (Fig. 1A). For the duration of the implantation, this tissue becomes the recipient of silicone particles that are released from the implant. The presence of silicone particles in periprosthetic tissues was first reported in 1967[16] and remains a cause for concern today. There are three potential sources of silicone particles that may combine to expose periprosthetic tissues (Fig. 1B). (i) *Surface debris* are solid fragments detaching from the cross-linked silicone elastomer shell due to implant surface wear and fatigue. This process is accentuated with increasing degree of surface texturing, namely macrotextured implants[17–20] (Fig. 1C). Breast implant debris demonstrate pro-inflammatory effects both *in vitro*[21] and *in vivo* in cell and animal model[22] for both innate (macrophage) and adaptive (lymphocytes) mediated inflammation (reviewed in[17]). (ii) *Silicone gel permeation* refers to the diffusion of non-reticulated low molecular-weight silicone species

confined within the filling gel through the elastomer shell of the breast implant. This physical process, often referred to in the literature under the misnomer "*gel bleed*", has been estimated at 300 mg per year per intact implant[23], a negligible amount from an aesthetic point of view but significant on a cellular scale. In the same vein and very recently, Danino *et al*. quantified the number of silicone particles in periprosthetic tissue from intact implants. They found an average of one million silicone particles per capsule[24]. (iii) *Rupture* of the implant envelope that triggers the leak of the silicone filling gel, which can be considered as an intensified form of gel bleed. In most cases, silicone leakage after rupture is confined to the periprosthetic capsule (intracapsular rupture) but can occasionally spread to the surrounding tissue if both the implant and capsule have been damaged (extracapsular rupture). In the literature, intracapsular rupture is typically described as "silent", *i.e* asymptomatic and clinically undetectable. It is considered to be a relatively benign condition[25] with no direct health risk[26,27], which together support the idea of silicone innocuity.

In short, the likelihood of periprosthetic tissue coming into contact with silicone during implantation is therefore highly significant. Accordingly, silicone particles embedded in periprosthetic tissue may be a potential source of chronic inflammation around breast implants. Here, we present a pilot study investigating the inflammatory characteristics of human periprosthetic tissue following silicone exposure. In particular, we focus on changes in (i) tissue organization and (ii) transcriptomic signatures of human periprosthetic tissues exposed to different sources of silicone with respect to implant integrity (intact or ruptured), surface texturing (macro- or microtexturing) and implant filling (silicone gel or serum). Overall, this work provides new insights into the immunological mechanisms triggered by silicone, and, once again, challenges the concept of silicone safety.

Materials and Methods

Tissue sampling and data collections

This pilot study was conducted between 2017 and 2023. Sampling of tissue explants was bi-centric and strictly performed on healthy women. Samples were collected from patients who had previously participated in our research[53] and from the tissue bank of Franche-Comté (reference BB-0033-00024) from the University Hospital of Besançon (France). When possible, histological sections were also collected. After approbation by the local institutional review board (NCT06414785), patients were required to provide informed consent to the use and analysis of their data. After anonymization of the patients, the following data were collected: (i) age of the patient (ii) characteristics of the breast implants, including volume, shape, manufacturer, filler (saline or silicone gel), surface topography (macrotextured and microtextured, see[53] for details) and implant integrity (intact versus ruptured). Implant integrity was assessed by the operating surgeon by macroscopic examination of the explanted device. (iii) specifications of the breast implant surgery including surgical approach, type of implant pocket, reason for explantation and duration of device implantation.

Histology and image acquisition

A total of 43 patients were included in the histological analyses. The relevant patient and data implant characteristics are gathered in Tab.1. Serial 4 µm-thick sections were obtained from formalin-fixed, paraffin-embedded breast capsule samples using a microtome, then stained with hematoxylin-eosin (HE) or hematoxylin-eosin-saffron (HES). Microscopic observations were done using a light microscope (Leica DM2000) with objectives of 20X, 40X and 63X. The micrographs were captured using a digital camera (LAS Version 4.2) and the photo layout was performed using

image software (Adobe, PhotoShop cc2019). The histological section analysis was performed by Novotec institute (Bron, France) in a blinded condition by a certified and trained histologist.

Implant categories (histology)	Ruptured	Macrotextured	Microtextured	Textured saline-filled	
Filling	Silicone gel			Saline	**Total sampling**
All implants (%)	15/43 (35%)	10/43 (23%)	13/43 (30%)	5/43 (12%)	43/43 (100%)
Patient age (year) Mean +/- SD	59 +/-15	59 +/-15	48 +/-19	54 +/-15	55 +/-16
Duration of implantation (year) (implantation to explantation) Mean +/- SD	14 +/- 8	12 +/-5	11 +/-6	13 +/- 4	13 +/-6
Implant volume mL +/- SD	335 +/-83	316 +/-84	241 +/- 57	192 +/- 45	278 +/-90
Implant shape					
• Round	5/15 (33%)	4/10 (40%)	7/13 (54%)	5/5 (100%)	21/43 (48%)
• Anatomic	6/15 (40%)	3/10 (30%)	5/13 (38%)	0/7 (0%)	14/43 (33%)
• Not reported	4/15 (27%)	3/10 (30%)	1/13 (8%)	0/7 (0%)	8/43 (19%)
Manufacturer					
• Allergan	3/15 (20%)	3/10 (30%)	0/9 (0%)	0/5 (0%)	6/43 (14%)
• Arion	2/15 (13%)	0/10 (0%)	0/9 (0%)	1/5 (20%)	3/43 (7%)
• Céréform	1/15 (7%)	1/10 (10%)	0/9 (0%)	0/5 (0%)	2/43 (5%)
• Mc Ghan	0/15 (0%)	0/10 (0%)	4/13 (31%)	0/5 (0%)	4/43 (10%)
• Mentor	1 /15 (7%)	0/10 (0%)	0/9 (0%)	0/5 (0%)	1/43 (3%)
• Perthèse	1/15 (7%)	0/10 (0%)	2/13 (15%)	0/5 (0%)	3/43 (7%)
• PIP	3/15 (20%)	0/10 (0%)	0/9 (0%)	0/5 (0%)	3/43 (7%)
• Sebbin	2/15 (13%)	5/10 (50%)	0/9 (0%)	0/5 (0%)	7/43 (16%)
• Silimed	0/15 (0%)	0/10 (0%)	5/13 (38%)	2/5 (40%)	7/43 (16%)
• Not reported	2/15 (13%)	1/10 (10%)	2/13 (15%)	2/5 (40%)	7/43 (16%)
Surgical approach					
• Flap edge	3/15 (20%)	2/10 (20%)	2/13 (15%)	0/5 (0%)	7/43 (18%)
• Mastectomy scar	4/15 (27%)	5/10 (50%)	1/13 (8%)	0/5 (0%)	10/43 (23%)
• Periareolar	7/15 (46%)	1/10 (10%)	6/13 (46%)	2/5 (40%)	16/43 (37%)
• inflamammary	0/15 (0%)	0/10 (0%)	0/13 (0%)	2/5 (40%)	2/43 (5%)
• Not reported	1/15 (7%)	2/10 (20%)	4/13 (31%)	1/5 (20%)	8/43 (18%)
Pocket					
• Under a flap	3/15 (20%)	0/10 (0%)	0/13 (0%)	0/7 (0%)	3/43 (8%)
• Prepectoral	3/15 (20%)	3/10 (30%)	5/13 (38%)	4/5 (80%)	15/43 (35%)
• Retropectoral	8/15 (53%)	2/10 (20%)	3/13 (23%)	0/5 (0%)	13/43 (30%)

• not reported	1/15 (7%)	5/10 (50%)	5/13 (38%)	1/5 (20%)	12/43 (28%)
Indications for explantation					
• Rupture	15/15(100 %)	0/10 (0%)	0/13 (0%)	0/5 (0%)	15/43 (35%)
• Suspicion of rupture	0/15 (0%)	1/10 (10%)	0/13 (0%)	0/5 (0%)	1/43 (3%)
• revision surgery	0/15 (0%)	2/10 20%)	1/13 (8%)	3/5 (60%)	6/43 (14%)
• controlateral complication	0/15 (0%)	5/10 (50%)	10/13 (56%)	0/5 (0%)	15/43 (35%)
• Size change/implant removal	0/15 (0%)	2/10 (20%)	1/13 (8%)	0/5 (0%)	3/43 (7%)
• Not reported	0/15 (0%)	0/10 (0%)	1/13 (8%)	2/5 (40%)	3/43 (7%)

Tab 1. Collection of patients, surgical and implant data for histology sampling.

Scoring of inflammation in histological sections

An inflammatory scoring system based on semi-quantitative data obtained from tissues was established in blinded condition. The scoring approach was derived from the quantification of (i) immune cells in each tissue, including polymorphonuclear cells, lymphocytes, macrophages, foamy macrophages and foreign body giant cells, (ii) silicone identification and (iii) synovial-like metaplasia. The scale for each variable was as follows: frequency of observation: score = 0: absence; score=1 limited; score=2: moderate; score=3: severe. FBR is mainly driven by macrophage cells[54] and thus, total FBR inflammation per tissue was calculated by summing the scores obtained with macrophages, foamy macrophages and foreign body giant cells. The resulting scores were then categorized as follow: score = 0: no inflammation; 1≤score≤3: limited inflammation; 4≤score≤6: moderate inflammation; 6≤score≤9: severe inflammation. The frequency of each variable was calculated in terms of percentage for the four categories, *i.e* ruptured, macro-, microtextured and saline-filled implants (number of samples with variable / total number of samples x 100). Histology scoring profiles were generated by using Plotly software (Plotly Montreal Quebec Canada) and included mean values, standard error of the mean, and

putative outliers. The statistical analyses included a *t* test with levels of significance ranging from p<0.01 (*), p<0.001 (**) and p<0.0001 (***).

Tissue disruption, RNA extraction, RNAseq

The collected tissues were immediately immersed in RNAlater solution (Invitrogen, Carlsbad, Calif.) and preserved at -20 °C until further use. Total RNAs were extracted using the RNeasy Fibrous Tissue Mini Kit (Qiagen) in accordance with the manufacturer's instructions. The tissues were weighed to 25 ± 5 mg, then cut into small pieces with a scalpel, and finally transferred to 2mL tubes containing beads (CKMIX 28R, Bertin Instruments; Rockville, MD, USA) pre-filled with 300µL lysis buffer. The tubes containing the tissue were then placed in a tissue homogenizer (Precellys Evolution, Bertin Instruments Tustin, USA) where the tissue was mechanically ground to a liquid twice at 8500 rpm for 30 seconds. Following proteinase K treatment, samples were transferred to columns for RNA purification, including a DNAse treatment. RNA concentration and quality were evaluated on Bioanalyzer (Agilent). Twenty-one RNAs met the quality requirements for RNA sequencing, with a relative integrity number (RIN) greater than or equal to seven. Further details, including patient and implant characteristics are presented in Tab.2.

Implant categories (RNAseq)	**Ruptured**	**Macrotextured**	**Microtextured**	**Textured Saline-filled**	
Filling	Silicone gel			Saline	**Total sampling**
All implants (%)	8/21 (38%)	5/21 (24%)	5/21 (24%)	3/21 (14%)	21/21(100%)
Patient age (year) Mean +/- SD	49 +/-8	50 +/-8	43 +/-16	41 +/-7	47 +/-10
Duration of implantation (year) (implantation to explantation) Mean +/- SD	12 +/- 3	15 +/-1	7 +/-6	13 +/-4	12 +/-5
Implant volume	378 +/- 114	276 +/-27	217 +/-67	302 +/- 121	300 +/-102

mL +/- SD					
Implant shape					
• Round	3/8 (38%)	4/5 (80%)	2/5 (40%)	1/3 (33%)	10/21 (48%)
• Anatomic	3/8 (38%)	1/5 (20%)	0/5 (0%)	1/3 (33%)	5/21 (24%)
• Not reported	2/8 (24%)	0/5 (0%)	3/5 (60%)	1/3 (33%)	6/21 (28%)
manufacturer					
• Allergan	1/8 (13%)	5/5 (100%)	0/5 (0%)	1/3 (33%)	7/21 (33%)
• Arion	0/8 (0%)	0/5 (0%)	0/5 (0%)	1/3 (0%)	1/21 (5%)
• Céréform	0/8 (0%)	0/5 (0%)	0/5 (0%)	0/3 (33%)	0/21 (0%)
• Eurosilicone	0/8 (0%)	0/5 (0%)	0/5 (0%)	1/3 (0%)	1/21 (5%)
• Nagor	1/8 (13%)	0/5 (0%)	2/5 (40%)	0/3 (0%)	3/21 (14%)
• Polytech	0/8 (0%)	0/5 (0%)	0/5 (0%)	0/3 (0%)	0/21 (0%)
• Sebbin	6/8 (75%)	0/5 (0%)	0/5 (0%)	0/3 (0%)	6/21 (29%)
• Not reported	0/8 (0%)	0/5 (0%)	3/5 (60%)	0/3 (0%)	3/21 (14%)
Surgical approach					
• Transaxillary	0/8 (0%)	3/5 (60%)	0/5 (0%)	0/3 (0%)	3/21 (14%)
• Mastectomy scar	0/8 (0%)	0/5 (0%)	0/5 (0%)	0/3 (0%)	0/21 (0%)
• Periareolar	1/8 (13%)	2/5 (40%)	2/5 (40%)	3/3 (100%)	8/21 (38%)
• inflamammary	3/8 (38%)	0/5 (0%)	2/5 (40%)	0/3 (0%)	5/21 (24%)
• Not reported	4/8 (50%)	0/5 (0%)	1/5 (20%)	0/3 (0%)	5/21 (24%)
pocket					
• Under a flap	3/8 (38%)	5/5 (100%)	2/5 (40%)	1/3 (33%)	11/21 (52%)
• Prepectoral	2/8 (25%)	0/5 (0%)	2/5 (40%)	1/3 (33%)	5/21 (24%)
• not reported	3/8 (38%)	0/5 (0%)	1/5 (20%)	1/3 (33%)	5/21 (24%)
Reasons for explantation					
• Rupture	8/8 (100%)	0/5 (0%)	0/5 (0%)	0/3 (0%)	8/21 (38%)
• revision surgery	0/8 (0%)	3/5 (60%)	1/5 (20%)	1/3 (25%)	5/21 (24%)
• controlateral complication	0/8 (0%)	1/5 (20%)	2/5 (40%)	2/3 (75%)	5/21 (24%)
• Size change/implant removal	0/8 (0%)	0/5 (0%)	0/5 (0%)	0/3 (0%)	0/21 (0%)
• Not reported	0/8 (0%)	1/5 (20%)	2/5 (40%)	0/3 (0%)	3/21 (14%)

Tab 2. Collection of patients, surgical and implant data for RNA sequencing sampling.

RNAseq library

Library preparation was performed at the GenomEast platform at the Institute of Genetics and Molecular and Cellular Biology (Strasbourg, France) using Illumina Stranded mRNA Prep Ligation

- Reference Guide - PN 1000000124518. RNA-Seq libraries were generated from 100 ng of total RNA using Illumina Stranded mRNA Prep, Ligation kit and IDT for Illumina RNA UD Indexes Ligation (Illumina, San Diego, USA) according to manufacturer's instructions. Following polyA selection, mRNAs were fragmented at 94°C for 8 minutes. DNA libraries were amplified using 12 cycles of PCR. Surplus PCR primers were further removed by two successive purifications using SPRIselect beads (Beckman-Coulter, Villepinte, France). The final libraries were checked for quality and quantified using Bioanalyzer 2100 system (Agilent technologies, Les Ulis, France). Libraries were sequenced on an Illumina NextSeq 2000 sequencer as single read 50 base reads. Image analysis and base calling were performed using RTA version 2.7.7 and BCL Convert version 3.8.4. Reads were preprocessed using cutadapt version 4.2 to remove adapter[55], polyA and low-quality sequences (Phred quality score below 20), reads shorter than 40 bases were discarded for further analysis. Reads mapping to rRNA were also discarded (this mapping was performed using bowtie version 2.2.8[56]). Reads were then mapped onto the GRCh38 human genome assembly using STAR version 2.7.10b[57]. Gene expression was quantified using htseq-count version 0.13.5[58]and gene annotations from Ensembl release 110.

Differentially expressed gene analysis

Differential gene expression analysis was performed using the method for differential analysis of count data proposed by Love et al[59] and implemented in the Bioconductor package DESeq2 version 1.34.0 with a Wald test. Differentially expressed genes with absolute values of log2 (fold change) > 1 and adjusted *p-value* <0.05 were selected for further analysis, with *p-value* calculated according to the Benjamini and Hochberg *p-value* adjustment method[60]. Up- or downregulated transcripts were illustrated as Venn diagram and bar plot in all conditions using data visualization

tool available online (http://www.bioinformatics.com.cn/srplot). The transcriptomic data source will be available in a GEO repository, which is currently being prepared.

Biological and pathway-based enrichment analysis

To gain a deeper insight into the functional implication of the observed gene expression changes and to identify the key genes regulated by silicone exposure and/or surface topography, we performed a Gene Ontology (GO) term enrichment analysis and Kyoto Encyclopedia of Genes and Genomes (KEGG) annotations (see (36)). We have implemented all the genes that are specifically up- or down-regulated. We used g:Profiler (version e111_eg58_p18_30541362, https://biit.cs.ut.ee/gprofiler/gost) adjusted for "*Homo sapiens*", applied the Benjamini and Hochberg correction for multiple testing and a significance threshold of 0.05. Annotations were considered significant based on a concurrent *p-value* <0.05 and gene pool size >10, and were selected for display in a GO plot or GO chord representation. Online resources were used to create Venn diagrams (https://www.bioinformatics.com.cn/static/others/jvenn_en/example.html), bar charts (https://chart-studio.plotly.com), GO, KEGG enrichment and chord diagrams (https://biit.cs.ut.ee/gprofiler/gost and http://www.bioinformatics.com.cn/en). The figures were then annotated in Adobe Illustrator (CC 2019).

Results

Inflammation markers are limited in saline-filled and silicone gel-filled microtextured implants

Irrespective of the topography of the implant surface, whether micro- or macrotextured, the fibrotic capsular tissue that developed in contact with the saline-filled implants consisted of a dense and homogeneous matrix of collagen fibers and fibroblasts (Fig. 2A). Scattered macrophages were seen along the capsule in most specimens. Rare foreign body giant cells (Fig.

2B) and discrete foamy macrophages (observed in one patient) were identified in these tissues, testifying of silicone exposure originating specifically from the implant shell. Otherwise, no immune cell other than macrophages were found (Fig. 3A). In these tissues, the mean inflammation score was limited (1.8 ± 0.7, Fig. 3B). The fibrous tissue adjacent to the silicone gel-filled microtextured implants showed an organization similar to that of the saline-filled implants (Fig. 2C). Most of the immune cells were macrophages, mainly distributed at the implant interface. In some cases, macrophage-like cells were arranged in a synovial metaplasia-like manner[28–33] (Fig. 2C and 2D). Foamy macrophages (Fig. 2E) and FBGCs were occasionally associated with infiltrates of discrete silicone droplets (~5µm in diameter). Sporadic lymphocytes were also observed (Fig. 3A). In these tissues, the mean inflammation score is limited and statistically similar to that elicited in saline-filled implants (1.6 ± 0.8, Fig. 3B).

Inflammation markers range from limited to moderate in silicone gel-filled macrotextured implants

The immune response to gel-filled macrotextured implants was heterogeneous from patient to patient. Collagen matrix remained predominant in tissues with limited inflammation score (score <3, Fig. 2F) and punctuated by FBGCs filled with thread-like structures of translucent amorphous refractile material previously referred as silicone[34] (Fig. 2G). Localized brown deposits in vacuoles indicate phagocytosis debris (Fig. 2H). A striking reorganization affected tissues with higher inflammation score (score >3, Fig. 3B). Capsular tissues were characterized by a significant vascularization and heterogenous collagen matrix. A prominent accumulation of macrophage cells accumulated at the interface with the implant, forming synovial-like metaplasia. Deeper into the tissue, macrophages spread out in high density, reminiscent of the immune reaction defined

elsewhere in the literature as silicone-induced granuloma[12] (Fig. 2I). FBGCs and macrophages, with their cytoplasm containing refractory material, actively attempted to degrade silicone (Fig. 2J-K). Overall, the frequency of observation of silicone, FGBCs and to a lesser extent of lymphocytes was increased compared to microtextured and saline-filled implants (Fig. 3A). The macrophage-driven inflammation score in tissues facing macrotextured implants ranged from limited to moderate (score >3) (Fig. 3B), and was statistically higher than in microtextured or saline-filled implants.

Chronic macrophage-driven FBR in response to implant rupture

Capsular tissues facing ruptured implants showed distinct cytologic aspects. Two patterns of organization were reported depending on the specimen but independent of the degree of texture of the implant surface. In one hand, typical connective tissue was replaced by palisade-like tissue formed by multiple layers of juxtaposed foamy macrophages extending up to ~ 500µm thick (Fig. 2L) and rimmed by collagenous stroma (Fig. 2M-N). Silicone was sequestered in droplets or in vacuoles of 20-30µm in diameter. On the other hand, foamy macrophages give way to an expanse of large vacuoles filled with refringent material (up to 250µm in diameter) scattered within the collagenous tissue (Fig. 2O) and surrounded by FBGCs or macrophages (Fig. 2P-Q). The size of the vacuoles appeared to follow a gradient, with the smallest vacuoles at the implant interface and the largest in the innermost part of the tissue (Fig. 2O). In addition to macrophages, which were widely represented, we also observed small lymphocyte loci and polymorphonuclear cells in some sections (data not shown). Finally, despite clinically verified implant rupture, we were unable to observe silicone in all tissues, four of which were silicone-free, suggesting a bias in the region selected for the observation, possibly at the time of tissue collection. Of interest, silicone-free tissues were associated with a low inflammation score (<3). Overall, tissues facing ruptured

implants were statistically more immunoreactive than non-ruptured implants with inflammation scores ranging from severe (> 6) to limited (>3) (Fig. 3B).

Effect of silicone exposure on gene expression

RNA sequencing analysis revealed differences in gene expression between tissues facing ruptured implants and tissues facing intact implants (Fig. 4A and volcano plots, Fig. S1). Regardless of surface topography, a total of 3993 differentially expressed genes (including 1629 up-regulated and 2364 down-regulated, Fig. 4A-B) were highlighted when comparing tissues facing intact serum-filled implants with tissues facing gel-filled ruptured implants. Importantly, 333 genes were found to be differentially expressed when comparing the implant rupture group as a function of surface topography, *i.e.* macro- versus microtextured implants, including 97 and 236 up- and down-regulated genes respectively. This strongly suggests that tissue response is determined by a cumulative effect between gel and surface topography. Therefore, to improve the robustness of our approach, we then compared ruptured and intact implants with the same surface topography. Specifically, we found 892 differentially expressed genes (including 217 up-regulated and 675 down-regulated) between gel-filled macrotextured ruptured versus intact implants and 434 differentially expressed genes (including 232 up-regulated and 202 down-regulated) between gel-filled ruptured implants and intact microtextured implants (Fig. 4A-B).

Silicone exposure affects gene expression and related functional pathways

The differential gene expression between gel-filled ruptured implants and intact serum-filled implants highlighted the global effect of silicone exposure on periprosthetic tissues, regardless of surface texture, with serum-filled implants used as our reference group for this study. A total of 967 GO terms and 30 KEGG were found (Fig. 4C). Silicone exposure after implant rupture was

found to affect the immune response, including both innate and adaptive immune responses. The activity of several immune cells was found to be affected after silicone exposure, including leukocytes (activation, chemotaxis, cytotoxicity), T cells (activation and regulation) and B cells. Pathways associated with cell death and the apoptotic process were also highlighted, along with important functions such as wound healing, tissue morphogenesis, angiogenesis or reactive oxygen species (ROS) metabolic processes. Correlated KEGG pathways enrichment emphasized phagosome formation or proteoglycans in cancer and revealed pathological pathways such as diabetic cardiopathy, ROS-driven chemical carcinogenesis or sclerosis (Fig. 4D). In complement, by specifically discriminating up- or downregulated genes, we also shed light on the positive regulation of cytokine production or modification targeting the major histocompatibility complex (MHC), among others. Furthermore, GO terms of up-regulated genes specifically were clearly associated with autoimmune thyroid disease or diabetes mellitus (Fig. S2). Finally, we established relationships between genes and terms based on GO chord representations (Fig. 4E). In particular, we found an upregulation in the expression of genes encoding metalloproteinases (*mmp1* and *mmp9*), onco-inflammatory markers (*tnfsf13*[35]) and other genes associated with autoimmune diseases and/or chronic inflammation such as *il18*[36]; *nlrc4*[37]**,** *blnk* [38] or *pycard* and *tnsfs14*, both previously identified as diagnostic markers for rheumatoid arthritis[39]. Finally, some genes such as *bcl6*, previously shown to be involved in B-cell lymphoma associated with breast implants[40], were found to be downregulated.

Combined effects of silicone exposure and surface topography differentially determine gene expression and associated functional pathways.

Differential gene expression between ruptured macrotextured and ruptured microtextured gel-filled implants revealed the combined effect of silicone exposure and surface topography on

periprosthetic tissues. Among the 125 GO terms identified (Fig. 5A), processes related to the immune response were significantly represented, including antigen binding, cytokine binding, adaptive immune response, B cell, lymphocyte and leukocyte-mediated immunity (Fig. 5B). A number of key genes involved in these pathways, such as *il6* encoding for a pro-inflammatory interleukin involved in chronic inflammation, autoimmune diseases and cancer(49), are shown in Fig. 5C. As we found that most of the genes were downregulated, we took the analysis further and looked at the set of downregulated and upregulated genes separately. We found that the downregulated genes mainly affect pathways related to B-cell activation, humoral response, phagocytosis recognition or antigen binding or hematopoietic lineage among others (Fig. S3).

Next, we compared the gene expression profile between ruptured and intact gel-filled implants according to the level of surface texture, *i.e.* macrotexture or microtexture. In the context of surface macrotexture, additional silicone exposure led to the dysregulation of a large number of processes (Fig. 5D). It included notably cellular response to chemical stimulus, regulation of apoptotic process and programmed cell death or cell morphogenesis. Interestingly, KEGG pathways revealed a relationship between the set of dysregulated genes and the occurrence of pathologies such as rheumatoid arthritis (Fig. 5E), and in particular genes involved in MHC (*HLA, tnfsf13, il18*) shown in Fig. 5F. GO enrichment analysis of the set of differentially up-regulated genes showed that antigen processing and presentation of peptide antigens, especially via MHC class II, and metabolic activity (e.g. lipase, hydrolase...) were affected. KEGG charts revealed some pathological pathways such as asthma, autoimmune thyroid disease or type I diabetes mellitus (Fig. S4).

In the context of gel-filled microtextured implants, exposure to silicone after rupture results in the activation of 920 pathways (Fig. 5G), including gene pathways associated with immune and inflammatory response, cytokine activity, leukocyte migration and chemotaxis, mononuclear cell migration, T-cell activation, thereby promoting innate and adaptive immune responses and phagocytosis. Cell death and apoptotic processes were also highlighted (Fig. 5H). KEGG enrichment analysis revealed the involvement of several pathways related to cytokine activity or toll-like receptor signaling, underlining the direct link with inflammatory diseases such as rheumatoid arthritis. Finally, patients with microtextured ruptured implants were found to overexpress genes associated with inflammation such as chemokines (*ccl2-4*), cytokines (*il1, il6, il21*), tumor necrosis factor 14 (*tnfsfs14*) and downregulate genes involved in master signaling pathways such as *tgfβ2* among others (Fig. 5I). To complete the picture, GO enrichment analyses and KEGG functional analyses of up or down-regulated genes specifically are provided in Fig. S5. Notably, silicone exposure after implant rupture was found to trigger functional pathways related to Type I diabetes mellitus, Toll-like receptor signaling pathway or autoimmune thyroid disease.

Overall, these results show that silicone exposure in the event of rupture has a more drastic immunogenic effect in a microtextured than in a macrotextured context. Taken together with the histological results, this suggests that macrotextured implants are inherently more immunoreactive. Furthermore, as indicated by the different genetic profile of macrotextured versus microtextured gel implants, the periprosthetic tissue response appears to correlate not only with silicone exposure but also at the level of topography.

Discussion

To better understand the impact of silicone exposure released from breast implants on the human host response *in vivo*, we chose to study the response of periprosthetic tissues in contact with ruptured silicone gel-filled implants. This model allowed us to assess the tissue response to massive silicone exposure, which can be considered as a form of enhanced silicone permeation. Given the association between surface texturing and the induction of pathological conditions such as BIA-ALCL[41], we also sought to assess the potential for an additive effect between surface texturing and gel exposure. Previous studies in both animal and human models have clearly demonstrated that implant texture differentially modifies the host response. Two studies used a high-throughput transcriptomic approach, in rats (RNA sequencing[42]) and rabbits/mice/humans (NanoString RNA analyses[43]). To avoid oversimplification of the central questions addressed in this work, a forthcoming publication will specifically focus on the comparison of topographies among themselves.

When implanted *in vivo*, silicone implants elicit a succession of complex cellular and molecular events known as FBR culminating in the formation of a fibrous capsule -the periprosthetic tissue- that isolates the implant from the rest of the body. Generally, FBR is considered complete with the formation of the fibrous capsule, 3 to 6 months after implantation. However, this vision of a stable system is seriously challenged by the underlying dynamics of the physicochemical mechanisms of silicone release associated with implant aging. Two major, non-exclusive phenomena come into play: (1) the silicone permeation, often referred to as "gel bleed", and (2) the process of surface fatigue, that generates surface debris, both of which ultimately alter surface properties[44]. In addition, because surface texturing increases the surface area of the shell, it is likely that increased texturing will also increase permeation events. Surface debris and

gel permeation products can pass through the implant shell, be transported in the periprosthetic fluids, and reach the periprosthetic tissue. Consequently, iterative and prolonged exposure to silicone over extended period of time leads to a chronic state of FBR. Despite an average implantation time of 13+/-6 years in our sample, we could observe the typical hallmarks of silicone FBR. Histological analyses, including tissue organization, inflammation score and immune cell population demonstrated that silicone exposure was associated with a panel of cellular and tissue changes, in agreement with prior reports[45]. The inflammation score was the lowest with serum-filled and gel-filled microtextured implants. The introduction of silicone gel as an implant filler was correlated with the observation of lymphocytes, while an increase in surface topography was correlated with a marked presence of silicone-promoting FBR features such as FBGCs, foamy cells, silicone-induced granuloma or synovial-like metaplasia. Implant rupture and subsequent silicone exposure correlated with a greater diversity and number of immune cells, associated with a higher FBR inflammatory score. The dynamics of the periprosthetic tissue response to silicone gel are difficult to ascertain *in vivo*. Indeed, the onset of rupture, and therefore the duration of silicone exposure, cannot be accurately determined. Similarly, the source of silicone -gel or surface debris- identified in the capsular section cannot be distinguished using current histologic techniques. Consequently, the question of a putative differential contribution of gel filling versus shell debris in silicone-related immune responses remains open. Two distinct phenotypes were observed in the tissue surrounding of ruptured implants. One phenotype showed an accumulation of foamy macrophages forming a palisade-like structure. The other phenotype showed a transition from foamy macrophages to large areas of optically empty silicone-filled vacuoles surrounded by macrophages. Macrophages are unable to digest silicone, so it is postulated that foamy macrophages die over time, releasing intracellular silicone that fuses to form the large silicone

inclusions seen in tissues, thereby maintaining the chronic stimulation of immune cells. This hypothesis is supported by RNA sequencing analyses that highlighted activation of gene pathways related to (programmed) cell death, apoptosis and phagocytosis in the context of gel-filled rupture (Fig. 4D, 5E and 5H). Therefore, the continuous and recurrent release of silicone, coupled with the inability to clear it, may exacerbate the chronic state of FBR and promote a persistent inflammatory infiltrate, ultimately leading to the activation of pathological immune pathways.

Silicone polymers are considered as physiologically inert and are therefore widely used in a variety of medical applications (microfluidic devices, facial reconstruction, heart valves...). Since their first implantation in 1962, the potential toxicity of silicone breast implants has been repeatedly questioned with no clear answer to end this ongoing controversy. As reported by Colaris *et al*[10], diseases associated with silicone breast implants were first documented in 1964 and have not changed over the past 30 years. Surprisingly, despite the formal association established between BIA-ALCl and macrotextured implants[41] together with the plethora of studies linking patients with silicone breast implants to the onset of a number of autoimmune diseases (e.g arthritis, fatigue, arthralgia), skepticism about putative silicone immunotoxicity remains pervasive. The lack of scientific evidence demonstrating a direct link between the use of breast implants and these pathologies mainly contributes to fuel this skepticism. Indeed, the majority of epidemiologic data refer to *potential* associations such as autoimmune/inflammatory disorders in breast implant patients and/or symptom relief after implant removal[8,46,47]. Here, we provide the first biological argument by comparing the transcriptomic profile of periprosthetic tissues collected from healthy women with ruptured and non-ruptured implants. Differential transcriptome analysis between tissues in contact with macrotextured and microtextured ruptured implants revealed a cumulative effect of (i) silicone exposure and (ii) variations in surface topography. This

variation in gene expression highlights the subtle regulation of the immune system, which is able to modulate its response according to the filling and surface parameters of the implant. In this context, it is likely that the immune system differentially perceives silicone permeates and surface debris and that they may act synergistically to potentiate immune responses.

Prior to this study, the fact that ruptures were clinically asymptomatic was considered to be an indicator of implant safety. Herein, transcriptomic analyses confirmed histologic observations demonstrating that silicone exposure induces the expression of multiple signaling pathways associated with the stimulation of various immune cells (leukocytes, lymphocytes, T cells and mononuclear cells), along with the induction of immune signaling involved in a variety of pathologies. The presence of silicone within the periprosthetic capsule is responsible for chronic inflammation linked to the continuous stimulation of immune cells (macrophages, T lymphocytes), as mentioned in prior works[48,49]. Comparison of ruptured versus intact implants, especially when in the case of serum-filled implants, revealed an altered expression of a number of biomarkers involved in: i) the inflammatory response such as interleukins (*il1, il6, il12, il17, il18, il21, il23, il32, tlr*), cytokines production (*ccl2-4*), antigen recognition (*hla*), ii) the dysregulation of key signaling pathways (*fgf, tgfβ, wnt*) and iii), various pathological conditions. Specifically, genes involved in pathological conditions associated with onco-inflammatory markers *(tnfsf13, Il18, il6),* had a proven association with autoimmune diseases and/or chronic inflammation *(il1, il6, il17, Il18, Il23, bcl6, tnfsf13, nlrc4),* diagnostic marker of rheumatoid arthritis *(pycard),* sclerosis, chemical carcinogenesis induced by reactive oxygen species produced by phagocytes[50], neurodegeneration pathways, thyroid hormone signaling pathway. Taken together, these clinical results are strikingly reminiscent of those previously reported [47]. The effects of silicone are presumed to be universal among silicone implants. The results of this study indicate that the

transcriptomic effects of silicone exposure are dependent on the implant category. This suggests that each implant type may trigger a specific pathogenic context. Somehow, this phenomenon is already illustrated by two severe breast implant related diseases, both of which requiring reoperation: (i) BIA-ALCL, which is almost exclusively associated with macrotextured silicone implants marketed by a particular manufacturer[51]and (ii) capsular contracture (capsule fibrosis), which is mainly associated with smooth implants[52].

The periprosthetic capsule is a newly formed and dynamic interface elaborated by the host body to isolate itself from an exogenous device that cannot be phagocytosed. Shell debris resulting from surface erosion and gel permeates permanently expose this tissue to immunogenic silicone. To prevent the deleterious spread of silicone to the rest of the body, this “tissue of vigilance” adapts by sequestrating silicone, remodeling its ECM organization and activating the immune system. Immune cells that are unable to degrade immobilized free silicone particles induce chronic inflammation, which is characterized by a very specific molecular signature. The associated dysregulation of gene expression paves the way for the development of immune-related pathologies. In short, if silicone breast implants are biocompatible, it seems urgent to recognize that their degradation products are immunogenic to the host organism. Future work on extended sampling will confirm this pioneering approach.

Conclusions

This prospective study warns that silicone exposure, even if clinically asymptomatic, is immunogenic. The inability of macrophages to degrade silicone exposes patients to latent inflammation, which is accompanied by the expression of a number of markers of autoimmune pathology, which in turn is likely to precede the development of chronic disease in predisposed

patients. It is of the utmost importance to consider filling and topography factors as having cumulative effects on the initiation and persistence of an inflammatory context in implant patients. In light of these considerations, we propose that existing large-scale clinical studies, which have thus so far yielded inconclusive results, be re-examined to establish an objective link between the various manufacturing parameters of breast implants and the potential diseases they may promote. Finally, we firmly believe in the necessity to homogenize manufacturing processes, raw materials and innovations in the filling and covering of implants in order to limit the multiplication of health risks associated with their use. We are convinced that industry standards and practices should evolve to ensure long-term patient safety.

Acknowledgments

We thank Dr Nathalie Bricout that collected samples in the framework of the French Government CIFRE program (grant CIFRE2015–0843) and Dr Franck Monnien for the storage of samples in the tumour bank of Besançon. This work was supported by the Agence Nationale de la Recherche ANR "Safe-implant" (ANR-22-CE19-0028-01) and by the Interdisciplinary Thematic Institute HiFunMat, as part of the ITI 2021-2028 program of the University of Strasbourg, CNRS and Inserm, funded by IdEx Unistra (ANR-10-IDEX-0002) and SFRI (STRAT'US project, ANR-20-SFRI-0012) under the framework of the French Investments for the Future Program. Sequencing was performed by the GenomEast platform, a member of the 'France Génomique' consortium (ANR-10-INBS-0009). Finally, we would like to express our sincere thanks to Dr Abraham Chemtob and Dr Hatice Mutlu for their enlightening discussions on the chemistry of silicones.

References

[1] F.T. Foroushani, K. Dzobo, N.P. Khumalo, V.Z. Mora, R. de Mezerville, A. Bayat, Advances in surface modifications of the silicone breast implant and impact on its biocompatibility

and biointegration, Biomaterials Research 2022 26:1 26 (2022) 1–27. https://doi.org/10.1186/S40824-022-00314-1.

[2] N. Stafford, FDA finds breast implants to be safe but calls for better follow-up., BMJ 343 (2011) 5664. https://doi.org/10.1136/bmj.d5664.

[3] C.J. Coroneos, J.C. Selber, A.C. Offodile, C.E. Butler, M.W. Clemens, US FDA Breast Implant Postapproval Studies: Long-term Outcomes in 99,993 Patients, Ann Surg 269 (2019) 30–36. https://doi.org/10.1097/SLA.0000000000002990.

[4] J. Kaplan, R. Rohrich, Breast implant illness: a topic in review, Gland Surg 10 (2021) 430–443. https://doi.org/10.21037/GS-20-231.

[5] E. de F.C. Fleury, The contradiction of breast implant illness, Gland Surg 10 (2021) 2081–2083. https://doi.org/10.21037/gs-21-135.

[6] J.W. Cohen Tervaert, N. Mohazab, D. Redmond, C. van Eeden, M. Osman, Breast implant illness: scientific evidence of its existence, Expert Rev Clin Immunol 18 (2022) 15–29. https://doi.org/10.1080/1744666X.2022.2010546.

[7] D.A. Magno-Padron, J. Luo, T.C. Jessop, J.W. Garlick, J.S. Manum, G.C. Carter, J.P. Agarwal, A.C. Kwok, A population-based study of breast implant illness, Arch Plast Surg 48 (2021) 353–360. https://doi.org/10.5999/aps.2020.02117.

[8] J.Y. Katsnelson, J.R. Spaniol, J.C. Buinewicz, F. V. Ramsey, B.R. Buinewicz, Outcomes of Implant Removal and Capsulectomy for Breast Implant Illness in 248 Patients, Plast Reconstr Surg Glob Open 9 (2021) E3813. https://doi.org/10.1097/GOX.0000000000003813.

[9] S.K. Fuzzard, R. Teixeira, R. Zinn, A Review of the Literature on the Management of Silicone Implant Incompatibility Syndrome, Aesthetic Plast Surg 43 (2019) 1145–1149. https://doi.org/10.1007/s00266-019-01407-4.

[10] M.J.L. Colaris, M. de Boer, R.R. van der Hulst, J.W. Cohen Tervaert, Two hundreds cases of ASIA syndrome following silicone implants: a comparative study of 30 years and a review of current literature, Immunol Res 65 (2017) 120–128. https://doi.org/10.1007/s12026-016-8821-y.

[11] V. Borba, A. Malkova, N. Basantsova, G. Halpert, L. Andreoli, A. Tincani, H. Amital, Y. Shoenfeld, Classical Examples of the Concept of the ASIA Syndrome, Biomolecules 10 (2020) 1436. https://doi.org/10.3390/biom10101436.

[12] E. De Faria Castro Fleury, G.S. D'Alessandro, S.C.L. Wludarski, Silicone-induced granuloma of breast implant capsule (SIGBIC): Histopathology and radiological correlation, J Immunol Res 2018 (2018). https://doi.org/10.1155/2018/6784971.

[13] E. de Faria Castro Fleury, Breast Implant-Associated Anaplastic Large Cell Lymphoma (BIA-ALCL): An Open Wound, Aesthetic Plast Surg 44 (2020) 627–629. https://doi.org/10.1007/s00266-019-01602-3.

[14] S.B. Glasberg, C.A. Sommers, G.T. McClure, Breast Implant-associated Squamous Cell Carcinoma: Initial Review and Early Recommendations, Plast Reconstr Surg Glob Open 11 (2023) E5072. https://doi.org/10.1097/GOX.0000000000005072.

[15] G. Tanay, G. Halpert, A. Dotan, K. Sharif, A.M. Tsur, I. Shefler, H. Heidecke, H. Amital, A. Tanay, Y.A. Mekori, Y. Shoenfeld, Allergic manifestations in women with silicone breast implants, Hum Immunol (2023) 110747. https://doi.org/10.1016/j.humimm.2023.110747.

[16] F.L. Ashley, S. Braley, T.D. Rees, D. Goulian, D.L. Ballantyne, The present status of silicone fluid in soft tissue augmentation, Plast Reconstr Surg 39 (1967) 411–420. https://doi.org/10.1097/00006534-196704000-00012.

[17] N.J. Hallab, L. Samelko, D. Hammond, The Inflammatory Effects of Breast Implant Particulate Shedding: Comparison with Orthopedic Implants, Aesthet Surg J 39 (2019) S36–S48. https://doi.org/10.1093/asj/sjy335.

[18] N.J. Hallab, L. Samelko, D. Hammond, Particulate Debris Released from Breast Implant Surfaces Is Highly Dependent on Implant Type, Aesthet Surg J (2021). https://doi.org/10.1093/asj/sjab051.

[19] C. Garabedian, R. Vayron, N. Bricout, R. Deltombe, K. Anselme, M. Bigerelle, In vivo damage study of different textured breast implants, Biotribology 23 (2020) 100133. https://doi.org/10.1016/j.biotri.2020.100133.

[20] L.H. Webb, V.L. Aime, A. Do, K. Mossman, R.C. Mahabir, Textured breast implants: A closer look at the surface debris under the microscope, Plastic Surgery 25 (2017) 179–183. https://doi.org/10.1177/2292550317716127.

[21] C. Onnekink, R.M. Kappel, W.C. Boelens, G.J.M. Pruijn, Low molecular weight silicones induce cell death in cultured cells, Sci Rep 10 (2020) 1–12. https://doi.org/10.1038/s41598-020-66666-7.

[22] J.C. Doloff, O. Veiseh, R. de Mezerville, M. Sforza, T.A. Perry, J. Haupt, M. Jamiel, C. Chambers, A. Nash, S. Aghlara-Fotovat, J.L. Stelzel, S.J. Bauer, S.Y. Neshat, J. Hancock, N.A. Romero, Y.E. Hidalgo, I.M. Leiva, A.M. Munhoz, A. Bayat, B.M. Kinney, H.C. Hodges, R.N. Miranda, M.W. Clemens, R. Langer, The surface topography of silicone breast implants mediates the foreign body response in mice, rabbits and humans, Nat Biomed Eng 5 (2021) 1115–1130. https://doi.org/10.1038/s41551-021-00739-4.

[23] L.T. Yu, G. Latorre, J. Marotta, C. Batich, N.S. Hardt, In vitro measurement of silicone bleed from breast implants, Plast Reconstr Surg 97 (1996) 756–764. https://doi.org/10.1097/00006534-199604000-00011.

[24] M.A. Danino, M. Dziubek, J. Dalfen, M. Bonapace-Potvin, L. Gaboury, J.P. Giot, R. Laurent, Silicone Particles in Capsules Around Breast Implants: An Investigation Into Currently Available Implants in North America, Aesthet Surg J (2023). https://doi.org/10.1093/ASJ/SJAD363.

[25] L.R. Hölmich, I.M. Vejborg, C. Conrad, S. Sletting, M. Høier-Madsen, J.P. Fryzek, J.K. McLaughlin, K. Kjøller, A. Wiik, S. Friis, Untreated silicone breast implant rupture, Plast Reconstr Surg (2004). https://doi.org/10.1097/01.PRS.0000128821.87939.B5.

[26] A.H. Chao, R. Garza, S.P. Povoski, A review of the use of silicone implants in breast surgery, Expert Rev Med Devices 13 (2016) 143–156. https://doi.org/10.1586/17434440.2016.1134310.

[27] C. Hillard, J.D. Fowler, R. Barta, B. Cunningham, Silicone breast implant rupture: A review, Gland Surg 6 (2017) 163–168. https://doi.org/10.21037/gs.2016.09.12.

[28] A.D. del Rosario, H.X. Bui, S. Petrocine, C. Sheehan, J. Pastore, J. Singh, J.S. Ross, True synovial metaplasia of breast implant capsules: A light and electron microscopic study, Ultrastruct Pathol 19 (1995) 83–93. https://doi.org/10.3109/01913129509014607.

[29] D.R. Chase, K.C. Oberg, R.L. Chase, R.L. Malott, D.A. Weeks, Pseudoepithelialization of Breast Implant Capsules, Int J Surg Pathol 1 (1994) 151–154. https://doi.org/10.1177/106689699400100301.

[30] L. Pantanowitz, K. Balogh, Breast implant capsule with synovial metaplasia, Breast Journal 9 (2003) 428. https://doi.org/10.1046/j.1524-4741.2003.09518.x.

[31] J.L. Stone, T. Boost, Cytological features of breast peri-implant synovial metaplasia, Acta Cytol 58 (2014) 511–513. https://doi.org/10.1159/000369054.

[32] S. Krishnanandan, A. Abbassian, A.K. Sharma, G. Cunnick, Capsular synovial metaplasia mimicking silicone leak of a breast prosthesis: A case report, J Med Case Rep 2 (2008) 1–3. https://doi.org/10.1186/1752-1947-2-277.

[33] J.A. Jiménez-Heffernan, C. Bárcena, P. Muñoz-Hernández, Cytological features of breast peri-implant papillary synovial metaplasia, Diagn Cytopathol 46 (2018) 769–771. https://doi.org/10.1002/dc.23947.

[34] R.M. Kappel, L.L. Boer, H. Dijkman, Gel Bleed and Rupture of Silicone Breast Implants Investigated by Light-, Electron Microscopy and Energy Dispersive X-ray Analysis of Internal Organs and Nervous Tissue, Clin Med Rev Case Rep (2016) 10–12. https://www.researchgate.net/publication/301286015%0AGel.

[35] R. Chen, X. Wang, Z. Dai, Z. Wang, W. Wu, Z. Hu, X. Zhang, Z. Liu, H. Zhang, Q. Cheng, TNFSF13 Is a Novel Onco-Inflammatory Marker and Correlates With Immune Infiltration in Gliomas, Front Immunol 12 (2021). https://doi.org/10.3389/FIMMU.2021.713757.

[36] S.K. Sedimbi, T. Hägglöf, M.C.I. Karlsson, IL-18 in inflammatory and autoimmune disease, Cellular and Molecular Life Sciences 70 (2013) 4795–4808. https://doi.org/10.1007/S00018-013-1425-Y/METRICS.

[37] B. Sundaram, T.D. Kanneganti, Advances in Understanding Activation and Function of the NLRC4 Inflammasome, Int J Mol Sci 22 (2021) 1–12. https://doi.org/10.3390/IJMS22031048.

[38] G. Jin, Y. Hamaguchi, T. Matsushita, M. Hasegawa, D. Le Huu, N. Ishiura, K. Naka, A. Hirao, K. Takehara, M. Fujimoto, B-cell linker protein expression contributes to controlling allergic and autoimmune diseases by mediating IL-10 production in regulatory B cells, J Allergy Clin Immunol 131 (2013). https://doi.org/10.1016/J.JACI.2013.01.044.

[39] X.L. Geng, Y. Sen Jiang, C.N. Zhao, Z.Z. Zhang, Y.L. Liu, P.J. Ding, Serum PYCARD may become a new diagnostic marker for rheumatoid arthritis patients, Eur J Med Res 29 (2024) 1–6. https://doi.org/10.1186/S40001-024-01813-8/TABLES/3.

[40] C. Larrimore, A. Jaghab, A Rare Case of Breast Implant-Associated Diffuse Large B-Cell Lymphoma, Case Rep Oncol Med 2019 (2019) 1–4. https://doi.org/10.1155/2019/1801942.

[41] A. Loch-Wilkinson, K.J. Beath, R.J.W. Knight, W.L.F. Wessels, M. Magnusson, T. Papadopoulos, T. Connell, J. Lofts, M. Locke, I. Hopper, R. Cooter, K. Vickery, P.A. Joshi, H.M. Prince, A.K. Deva, Breast Implant-Associated Anaplastic Large Cell Lymphoma in Australia and New Zealand: High-Surface-Area Textured Implants Are Associated with Increased Risk, Plast Reconstr Surg 140 (2017) 645–654. https://doi.org/10.1097/PRS.0000000000003654.

[42] Y. Chen, X. Zhou, S. Huang, Y. Lan, R. Yan, X. Shi, X. Li, Y. Zhang, Z. Lei, D. Fan, Effect of Microgroove Structure in PDMS-Based Silicone Implants on Biocompatibility, Front Bioeng Biotechnol 9 (2022) 793778. https://doi.org/10.3389/FBIOE.2021.793778/BIBTEX.

[43] J.C. Doloff, O. Veiseh, R. de Mezerville, M. Sforza, T.A. Perry, J. Haupt, M. Jamiel, C. Chambers, A. Nash, S. Aghlara-Fotovat, J.L. Stelzel, S.J. Bauer, S.Y. Neshat, J. Hancock, N.A. Romero, Y.E. Hidalgo, I.M. Leiva, A.M. Munhoz, A. Bayat, B.M. Kinney, H.C. Hodges, R.N. Miranda, M.W. Clemens, R. Langer, The surface topography of silicone breast implants mediates the foreign body response in mice, rabbits and humans, Nat Biomed Eng 5 (2021) 1115–1130. https://doi.org/10.1038/s41551-021-00739-4.

[44] C. Garabedian, R. Vayron, N. Bricout, R. Deltombe, K. Anselme, M. Bigerelle, In vivo damage study of different textured breast implants, Biotribology (2020). https://doi.org/10.1016/j.biotri.2020.100133.

[45] P.J. Van Diest, W.H. Beekman, J.J. Hage, Pathology of silicone leakage from breast implants, J Clin Pathol 51 (1998) 493–497. https://doi.org/10.1136/jcp.51.7.493.

[46] J.W. Cohen Tervaert, M.J. Colaris, R.R. van der Hulst, Silicone breast implants and autoimmune rheumatic diseases: myth or reality, Curr Opin Rheumatol 29 (2017) 348–354. https://doi.org/10.1097/BOR.0000000000000391.

[47] M.I. Caravantes-Cortes, E. Roldan-Valadez, R.D. Zwojewski-Martinez, S.Y. Salazar-Ruiz, A.A. Carballo-Zarate, Breast Prosthesis Syndrome: Pathophysiology and Management Algorithm, Aesthetic Plast Surg (2020). https://doi.org/10.1007/s00266-020-01663-9.

[48] G. Cappellano, C. Ploner, S. Lobenwein, S. Sopper, P. Hoertnagl, C. Mayerl, N. Wick, G. Pierer, G. Wick, D. Wolfram, Immunophenotypic characterization of human T cells after

in vitro exposure to different silicone breast implant surfaces, PLoS One 13 (2018). https://doi.org/10.1371/JOURNAL.PONE.0192108.

[49] D. Wolfram, E. Rabensteiner, C. Grundtman, G. Böck, C. Mayerl, W. Parson, G. Almanzar, C. Hasenöhrl, H. Piza-Katzer, G. Wick, T regulatory cells and TH17 cells in peri-silicone implant capsular fibrosis, Plast Reconstr Surg 129 (2012). https://doi.org/10.1097/PRS.0B013E31823AEACF.

[50] P.J. Vernon, D. Tang, Eat-Me: Autophagy, Phagocytosis, and Reactive Oxygen Species Signaling, Antioxid Redox Signal 18 (2013) 677. https://doi.org/10.1089/ARS.2012.4810.

[51] E. Swanson, BIA-ALCL: Comparing the Risk Profiles of Smooth and Textured Breast Implants, Aesthetic Plast Surg 47 (2023) 245–250. https://doi.org/10.1007/S00266-023-03329-8/METRICS.

[52] A. Gorgy, N. Barone, H. Nepon, J. Dalfen, J.I. Efanov, P. Davison, J. Vorstenbosch, Implant-based breast surgery and capsular formation: when, how and why?—a narrative review, Ann Transl Med 11 (2023) 385–385. https://doi.org/10.21037/ATM-23-131/RC.

[53] I. Brigaud, C. Garabédian, N. Bricout, L. Pieuchot, A. Ponche, R. Deltombe, R. Delille, M. Atlan, M. Bigerelle, K. Anselme, Surface texturization of breast implants impacts extracellular matrix and inflammatory gene expression in asymptomatic capsules, Plast Reconstr Surg 145 (2020) 542E-551E. https://doi.org/10.1097/PRS.0000000000006606.

[54] Z. Sheikh, P.J. Brooks, O. Barzilay, N. Fine, M. Glogauer, Macrophages, Foreign Body Giant Cells and Their Response to Implantable Biomaterials, Materials 8 (2015) 5671. https://doi.org/10.3390/MA8095269.

[55] M. Martin, Cutadapt removes adapter sequences from high-throughput sequencing reads, EMBnet Journal 17 (2011) 10. https://doi.org/10.14806/EJ.17.1.200.

[56] B. Langmead, S.L. Salzberg, Fast gapped-read alignment with Bowtie 2, Nat Methods 9 (2012) 357–359. https://doi.org/10.1038/NMETH.1923.

[57] A. Dobin, C.A. Davis, F. Schlesinger, J. Drenkow, C. Zaleski, S. Jha, P. Batut, M. Chaisson, T.R. Gingeras, STAR: ultrafast universal RNA-seq aligner, Bioinformatics 29 (2013) 15–21. https://doi.org/10.1093/BIOINFORMATICS/BTS635.

[58] S. Anders, P.T. Pyl, W. Huber, HTSeq--a Python framework to work with high-throughput sequencing data, Bioinformatics 31 (2015) 166–169. https://doi.org/10.1093/BIOINFORMATICS/BTU638.

[59] M.I. Love, W. Huber, S. Anders, Moderated estimation of fold change and dispersion for RNA-seq data with DESeq2, Genome Biol 15 (2014). https://doi.org/10.1186/S13059-014-0550-8.

[60] Y. Benjamini, Y. Hochberg, Controlling the False Discovery Rate: A Practical and Powerful Approach to Multiple Testing, J R Stat Soc Series B Stat Methodol 57 (1995) 289–300. https://doi.org/10.1111/J.2517-6161.1995.TB02031.X.

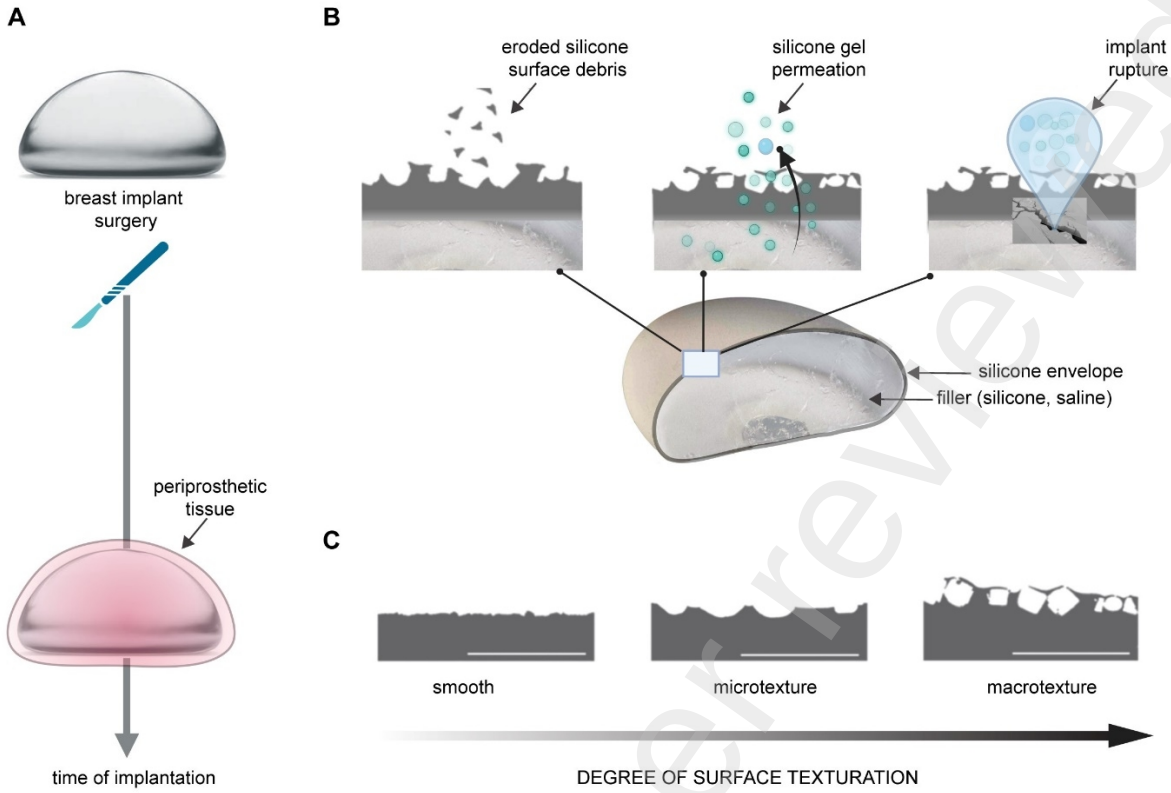

Figure_1 (**A**) Schematic representation of periprosthetic tissue surrounding breast implants, (**B**) Sources of silicone emanating from breast implants and (**C**) Illustration of breast implant surface topography (cross-section, scale bar = 1.0mm)

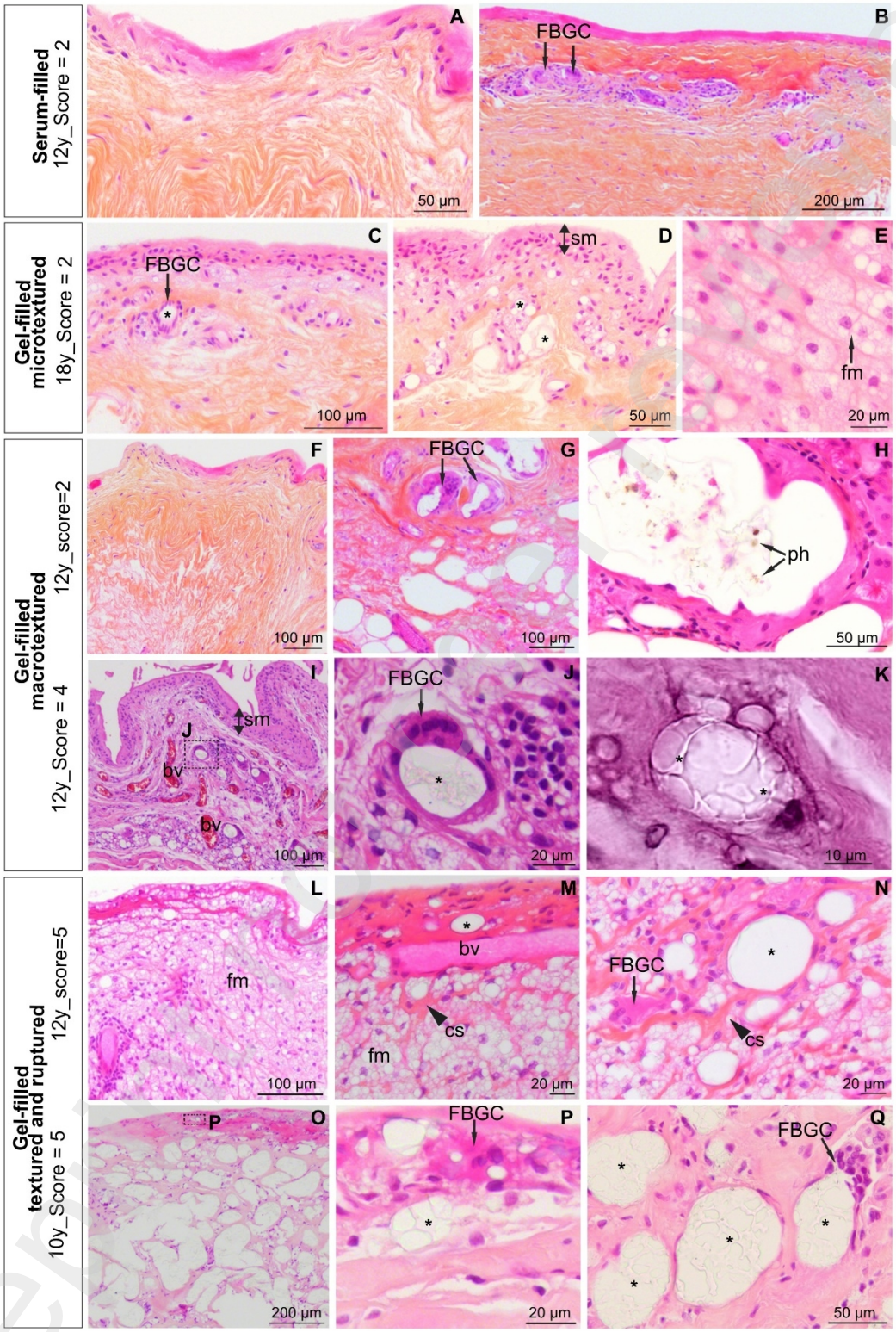

Figure_2 HES (hematoxylin eosin saffron)-stained breast implant periprosthetic tissue showing tissue response to different type of breast implants: serum-filled textured implants (**A, B**), gel-filled microtextured (**C-E**), gel-filled macrotextured implants (**F-K**) and gel-filled textured and ruptured implants (**L-Q**). Time of implantation and inflammation score for each condition is mentioned in lateral legend. *bv*: blood vessel, *cs*: collagen stroma, *sm*: synovial-like metaplasia, *fm*: foamy macrophage,

FGBC: foreign body giant cell, *ph*: phagocytosis residues. * indicates refractive material likely corresponding to silicone.

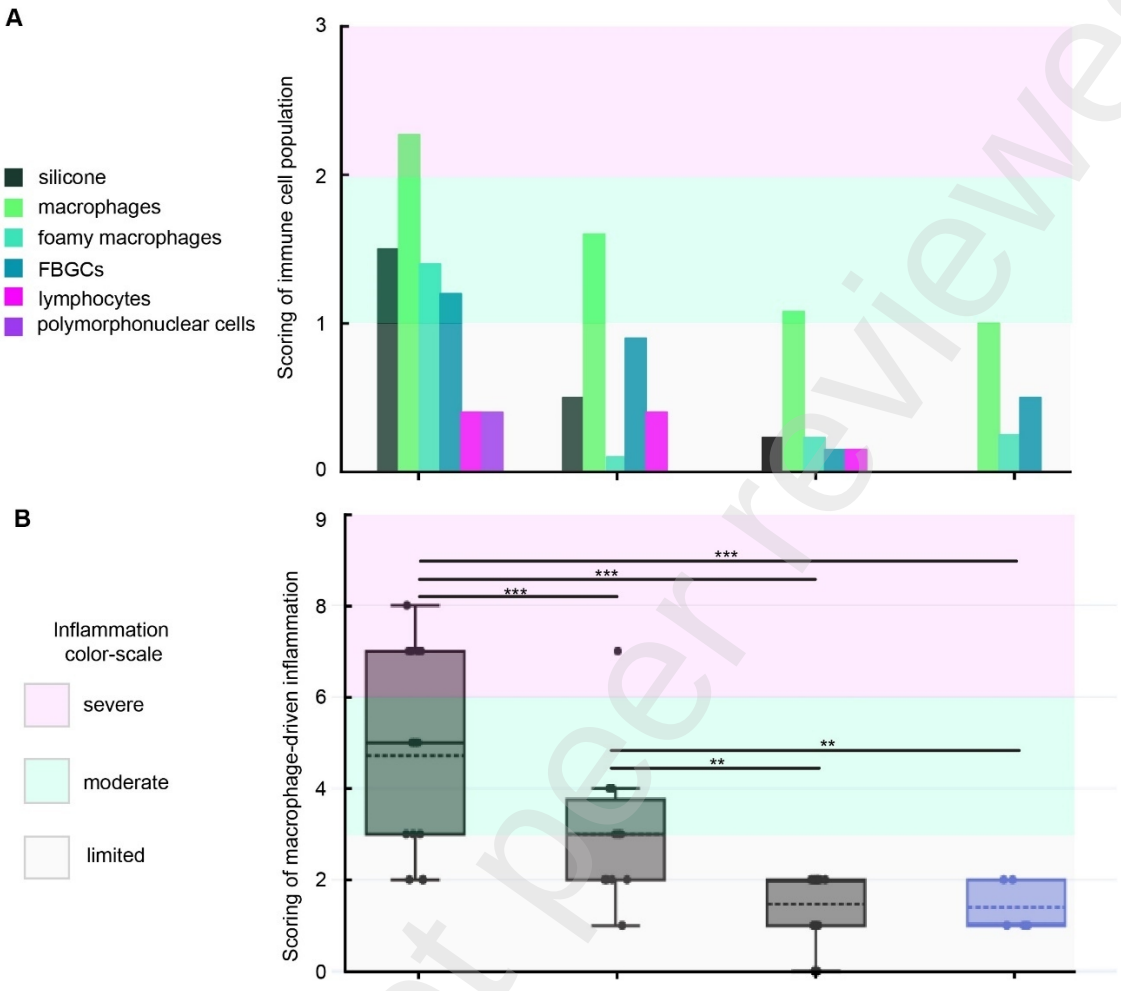

Implant integrity	ruptured	intact		
Implant filling	silicone gel			saline
Surface topography	mixed	macrotextured	microtextured	mixed
Mean inflammation scoring +/- SD	4.9 +/- 2.2	3.0 +/- 1.0	1.6 +/- 0.8	1.8 +/- 0.7

Figure_3 Quantification of inflammation in breast implant periprosthetic tissues as a function of implant integrity, surface texturing and filling in histology sampling. **A**, graph representing immune cell population based on their averaged frequency of observation. **B**, semi-quantitative scoring of macrophage cell-driven inflammation. ***p<0.0001; **p<0.01

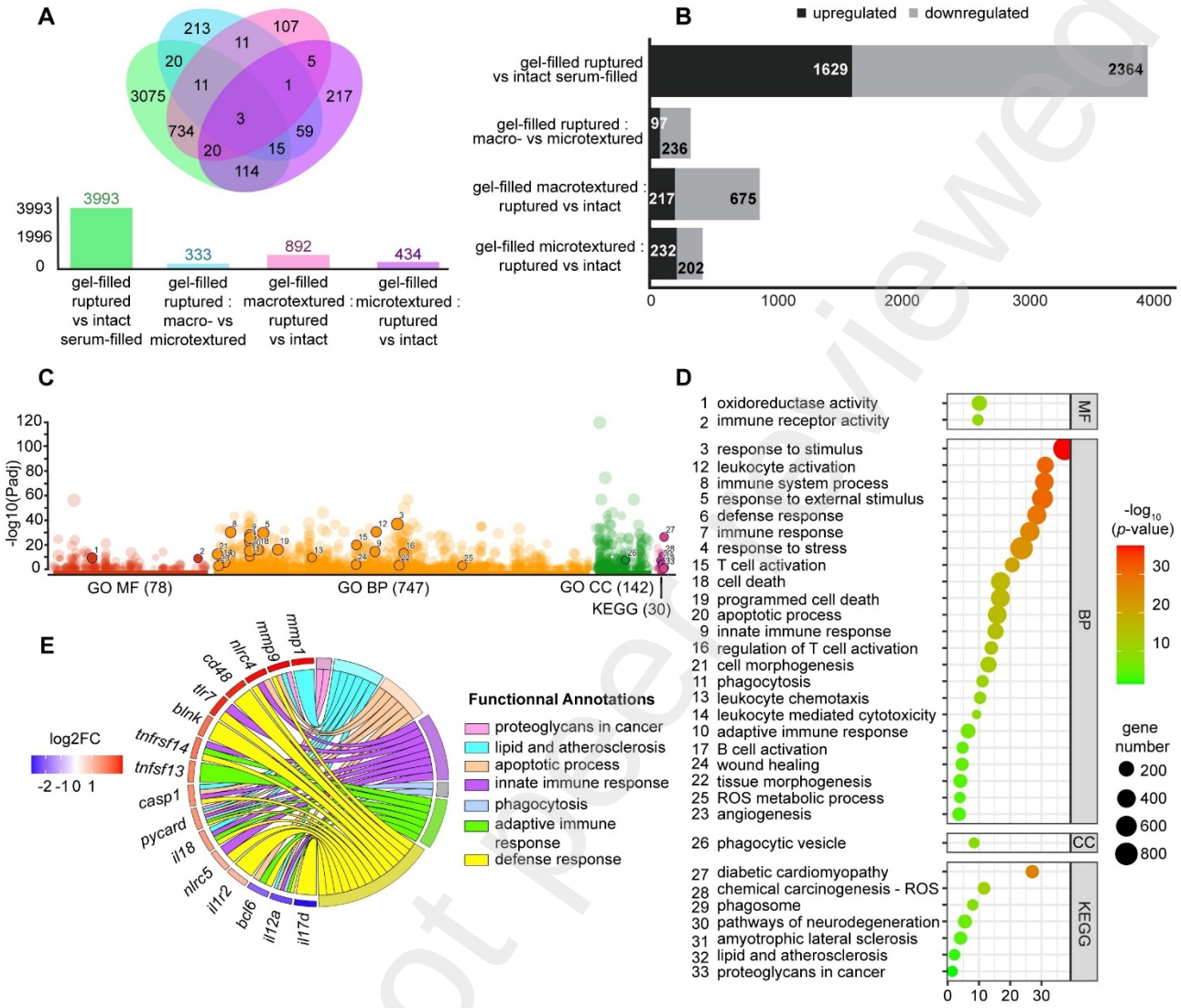

Figure_4 Effect of breast implant on gene expression in periprosthetic tissue regarding the different implant categories considered in this study. **A,** Venn diagram showing the total number of genes that are statistically differentially expressed in relation to the different categories. **B,** Bar chart showing the number of up- and down-regulated genes between the different categories. **C, D, E**, Focus on the effect of silicone gel exposure onto gene expression profile in periprosthetic tissue by comparing gel-filled ruptured implants and intact serum-filled implants. **C**, Complete GO enrichment analysis profile with gene sets colored into categories: GO MF (Molecular Function, red), GO BP (Biological Process, orange), GO CC (Cellular Component, green) and KEGG (pink). Numbered dots are emphasized in **D**. **D**, Bubble plot showing a selection of GO terms related to inflammation, cell death and diseases. GO terms in bold have been used to implement **E**. The size of the dot represents the number of genes contained in the gene set. **E,** GO chord plot showing the relationship between significantly differentially expressed genes and GO terms or KEGG pathways identified in **D**.

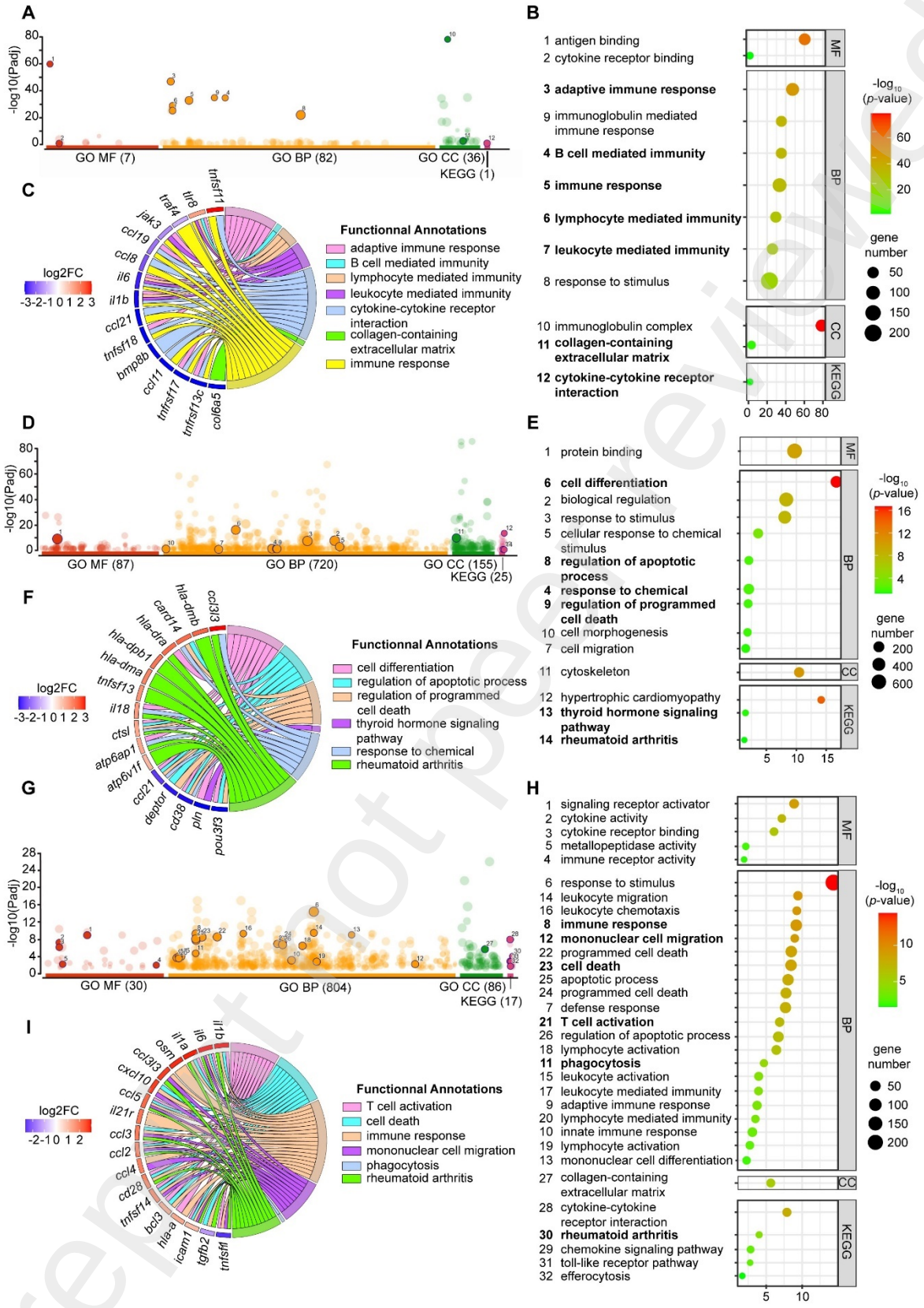

Figure_5 Effect of breast implant on periprosthetic gene expression as a function of implant integrity and surface topography. (**A-C**) Comparison of ruptured gel-filled macro- versus microtextured implants, (**D-F**) Comparison of ruptured versus intact gel-filled macrotextured implants, (**G-I**) Comparison of ruptured versus intact gel-filled microtextured implants. **A, D, G** Complete GO

enrichment analysis profile with gene sets colored into categories: GO MF (Molecular Function, red), GO BP (Biological Process, orange), GO CC (Cellular Component, green) and KEGG (pink). Numbered dots are emphasized in **B, E, H**, that display bubble plots showing a selection of GO terms related to inflammation, cell death, FBR and diseases. GO terms in bold have been used to implement **C, F, I,** GO chord plots showing the relationship between significantly differentially expressed genes and GO terms or KEGG pathways identified in B, E, H respectively.